Supporting Information

A dual functional probe for "turn-on" fluorescence response of Pb^{2+} and colorimetric detection of Cu^{2+} based on rhodamine derivative in aqueous media

Min Li,[a] Xiu-Juan Jiang,[a] Hui-Hui Wu,[a] Hong-Lin Lu,[a] Hai-Yang Li,[a] Hong Xu,*,[a] Shuang-Quan Zang,*,[a] and Thomas C. W. Mak[a,b]

[a] *College of Chemistry and Molecular Engineering, Zhengzhou University, Zhengzhou, 450001, P. R. China*

[b] *Department of Chemistry and Center of Novel Functional Molecules, The Chinese University of Hong Kong, Shatin, New Territories, Hong Kong SAR, People's Republic of China*

Author for correspondence:

E-mail: zangsqzg@zzu.edu.cn, xuhong@zzu.edu.cn

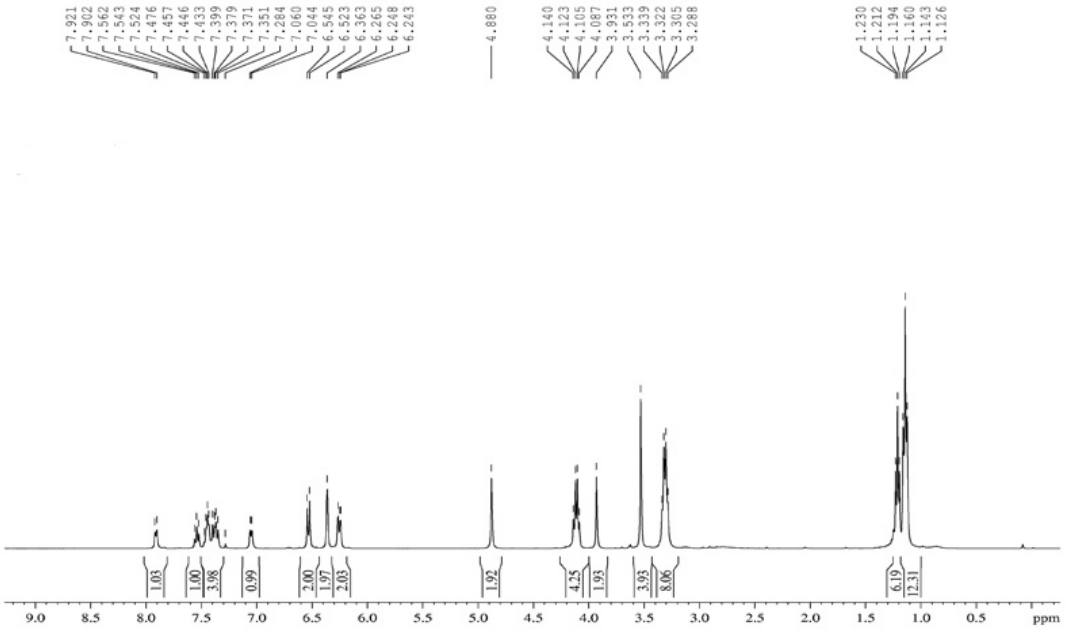

Fig. S1. ^{1}H NMR spectrum of **L** in $CDCl_3$.

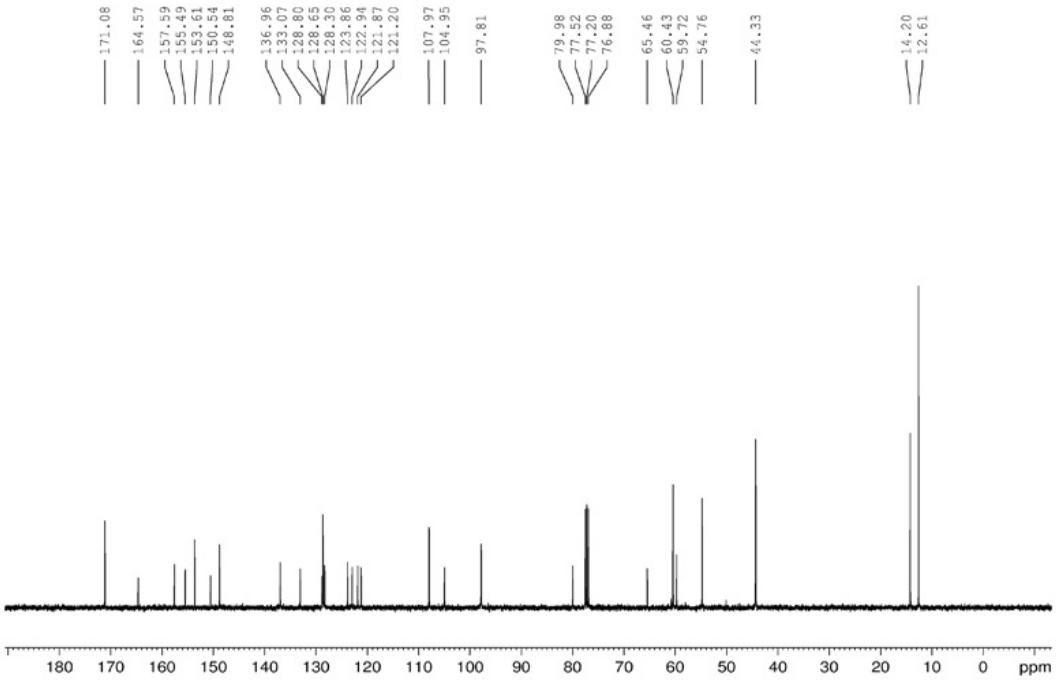

Fig. S2. ^{13}C NMR spectrum of **L** in $CDCl_3$.

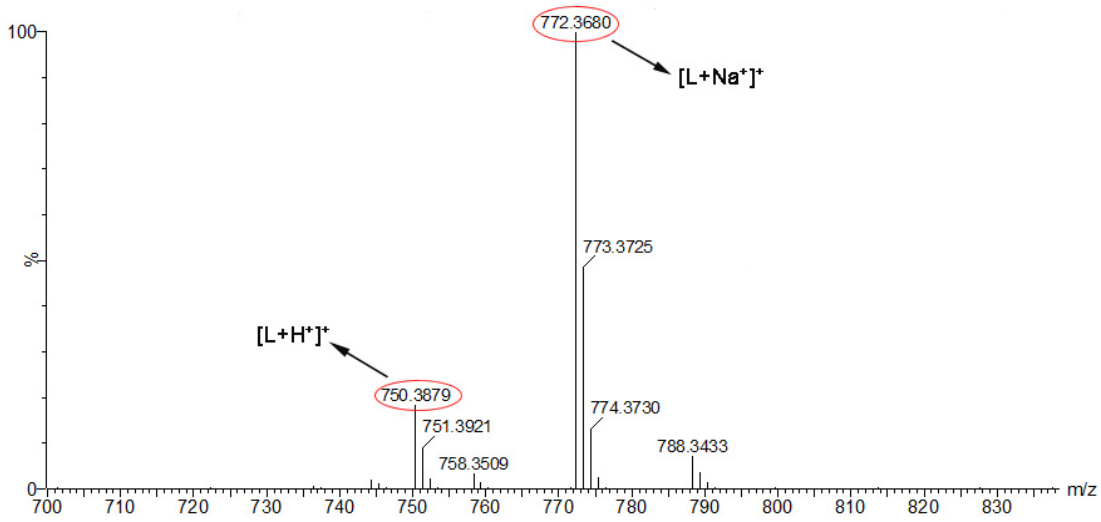

Fig. S3. ESI-MS spectrum of **L** in methanol.

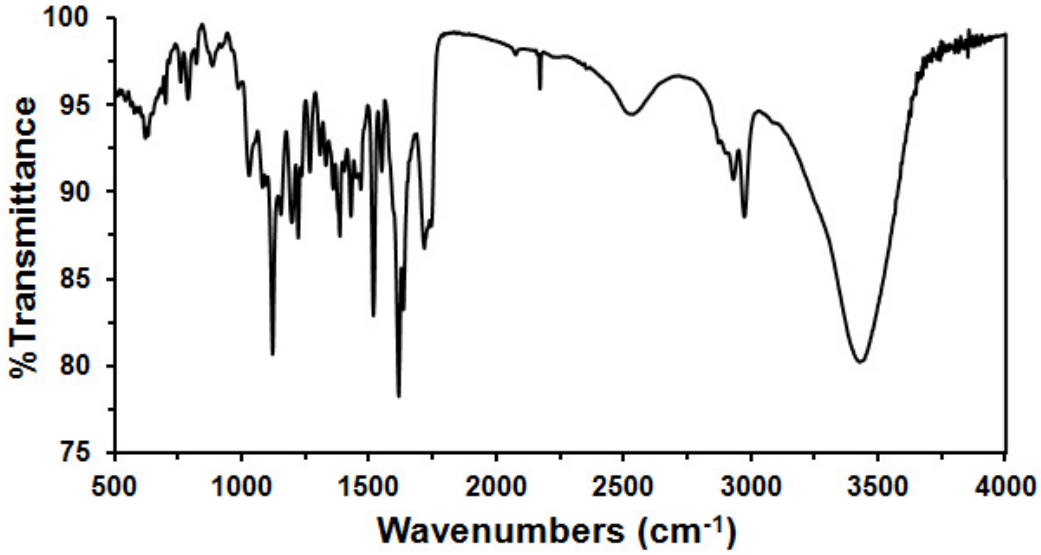

Fig. S4. IR spectrum of **L**.

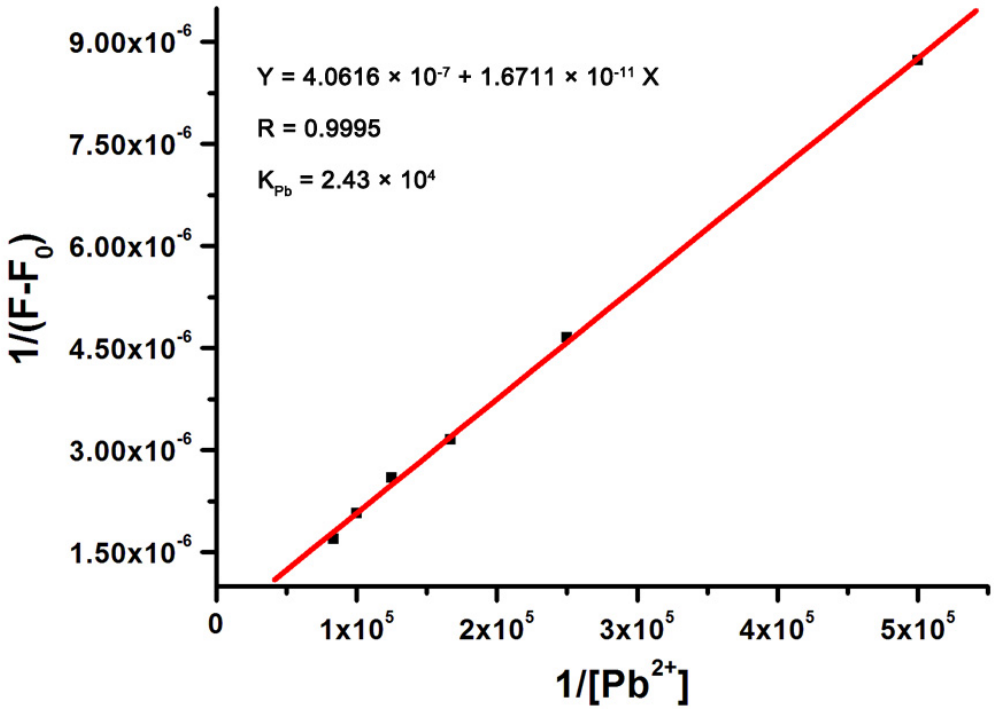

Fig. S5. Benesi–Hildebrand plot of **L** (10 μM) assuming 1:1 stoichiometry between **L** and Pb^{2+} in aqueous HEPES buffer (10 mM, pH 6.5) containing 1% CH_3CN (v/v). λ_{ex} = 483 nm. The binding constant of **L**-Pb^{2+} was 2.43×10^4 M^{-1}.

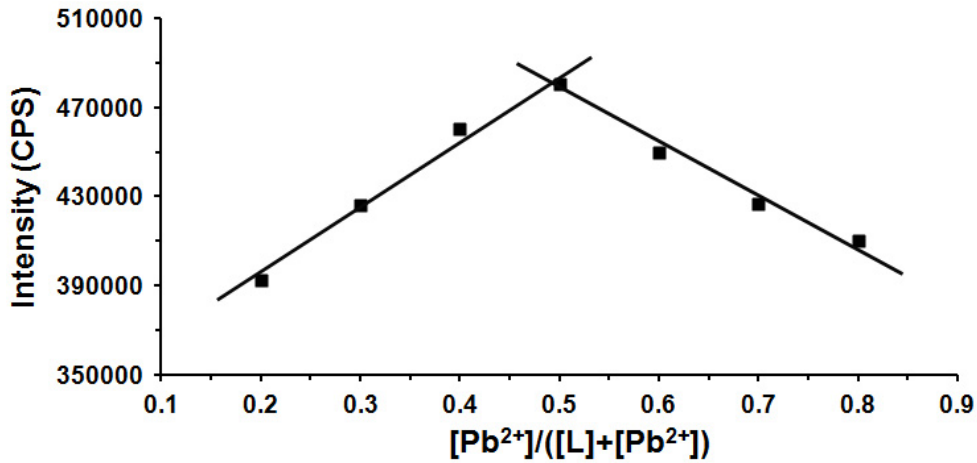

Fig. S6. Job's plot for **L** with Pb^{2+} in aqueous HEPES buffer (10 mM, pH 6.5) containing 1% CH_3CN (v/v).

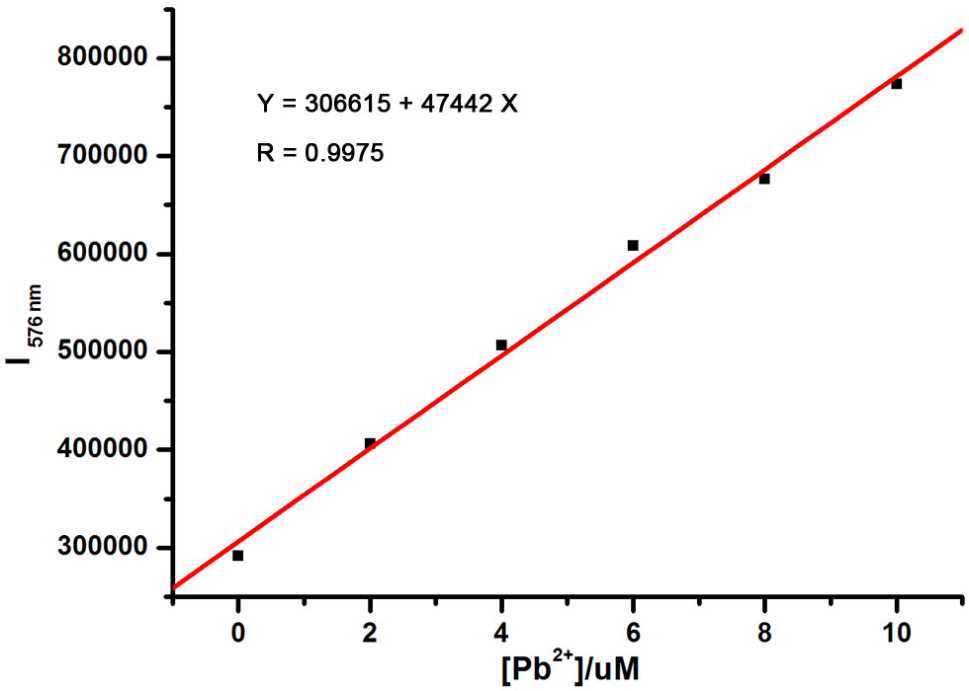

Fig. S7. The linearity of fluorescence intensity of **L** (10 μM) at 576 nm with respect to Pb^{2+} concentrations in aqueous HEPES buffer (10 mM, pH 6.5) containing 1% CH_3CN (v/v).

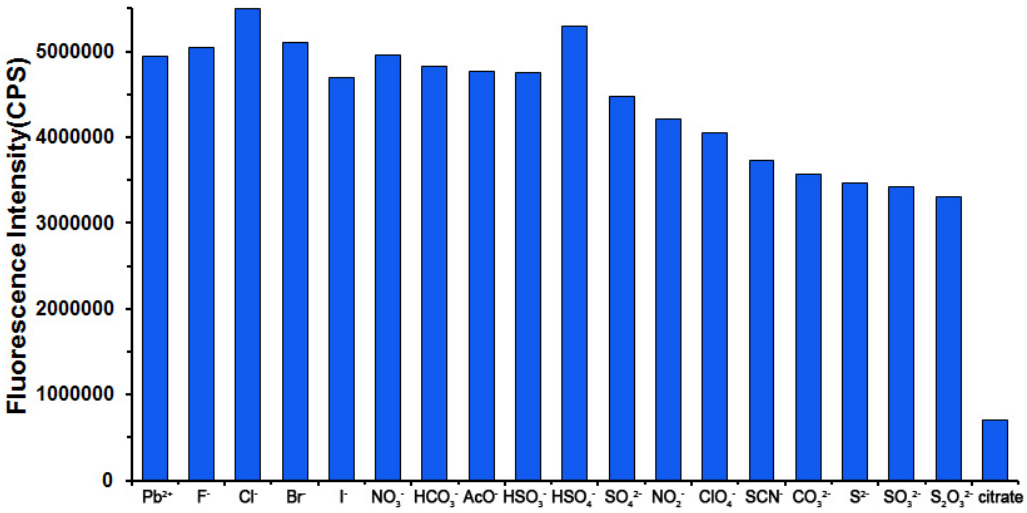

Fig. S8. Fluorescence responses (λ_{ex} = 483 nm) of **L** (10 μM) at 576 nm treated with marked anions (10 equiv) followed by 10 equiv Pb^{2+} in aqueous HEPES buffer (10 mM, pH 6.5) containing 1% CH_3CN (v/v).

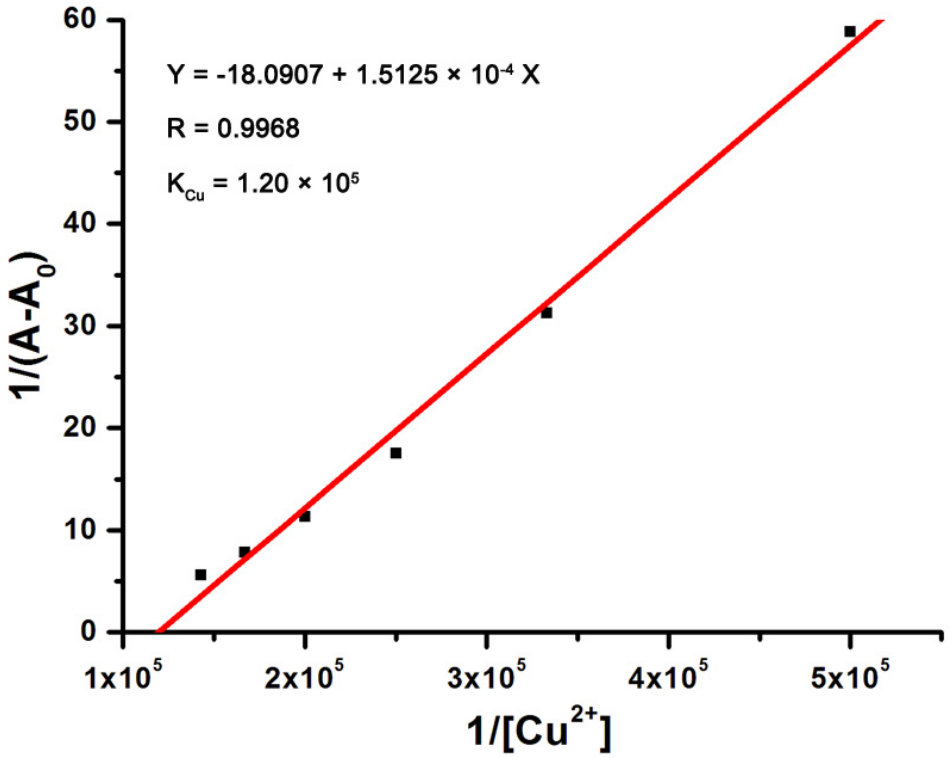

Fig. S9. Benesi–Hildebrand plot of **L** (10 μM) assuming 1:1 stoichiometry between **L** and Cu^{2+} in aqueous HEPES buffer (10 mM, pH 7.2) containing 1% CH_3CN (v/v). The binding constant of **L**-Cu^{2+} was 1.20×10^5 M^{-1}.

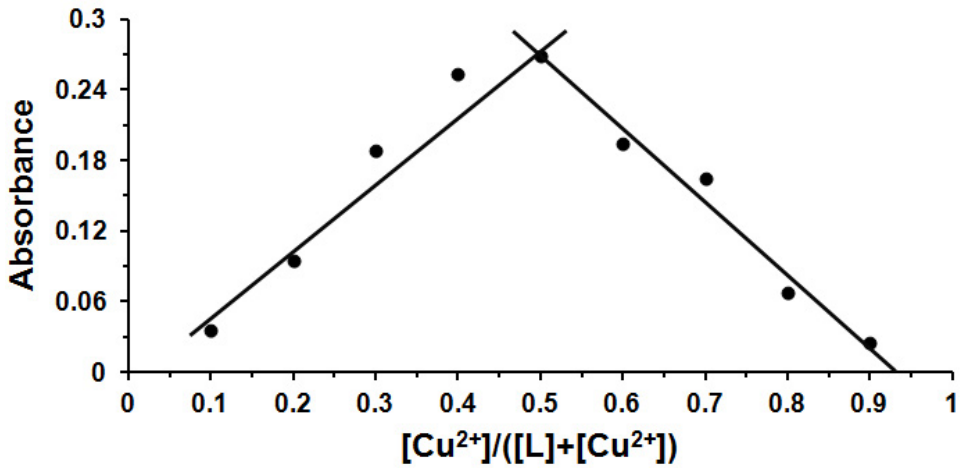

Fig. S10. Job's plot for **L** with Cu^{2+} in aqueous HEPES buffer (10 mM, pH 7.2) containing 1% CH_3CN (v/v).

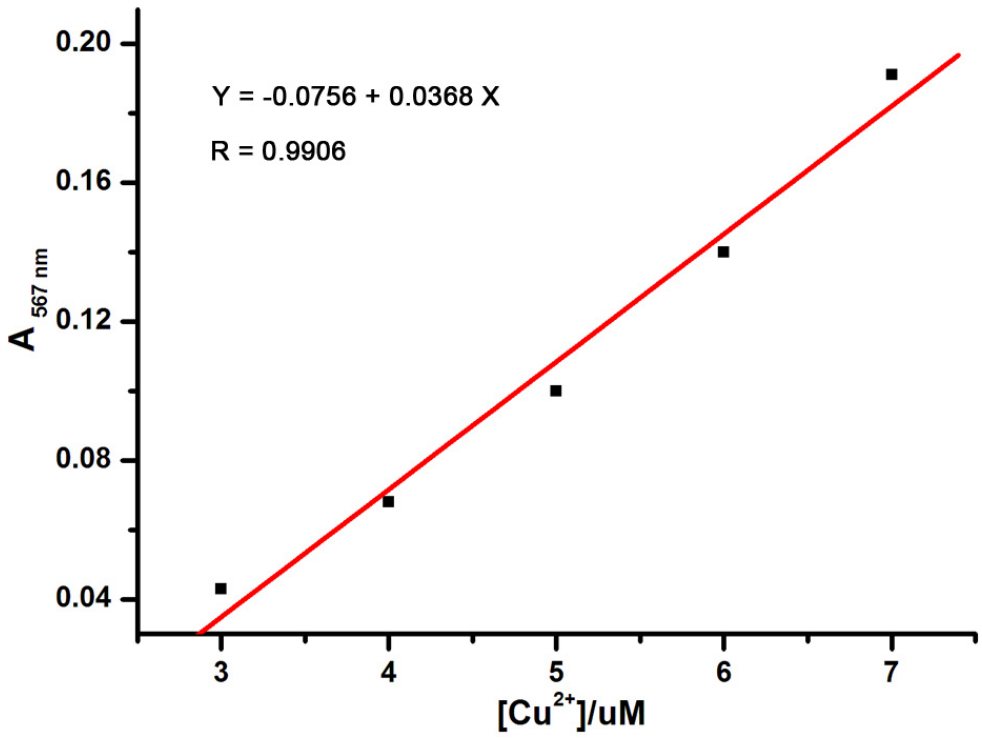

Fig. S11. The linearity of absorption intensity of **L** (10 μM) at 567 nm with respect to Cu^{2+} concentrations in aqueous HEPES buffer (10 mM, pH 7.2) containing 1% CH_3CN (v/v).

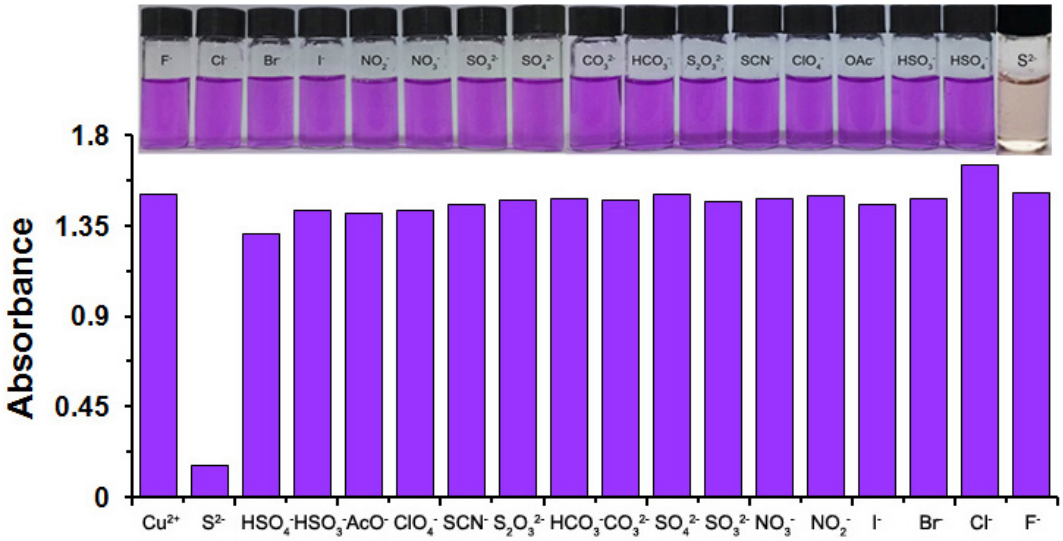

Fig. S12. Absorbance responses of **L** (10 μM) at 567 nm treated with marked anions (10 equiv) followed by 10 equiv Cu^{2+} in aqueous HEPES buffer (10 mM, pH 7.2) containing 1% CH_3CN (v/v). Inset: observed color changes of **L** (10 μM) treated with marked anions (10 equiv) followed by 10 equiv Cu^{2+}.

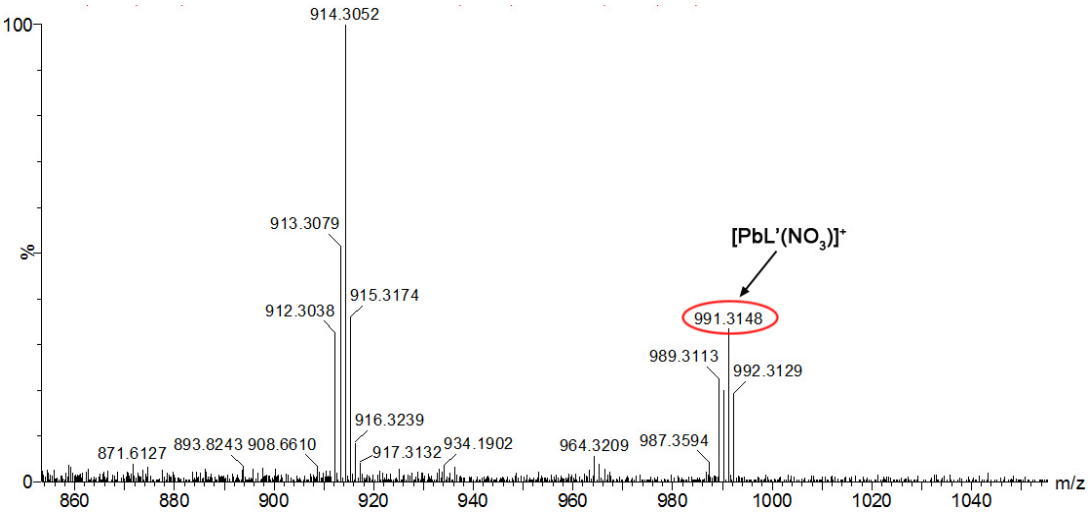

Fig. S13. ESI-MS spectrum of **L** in the presence of $Pb(NO_3)_2$, where **L**' represented the ester hydrolyzed product of **L**.

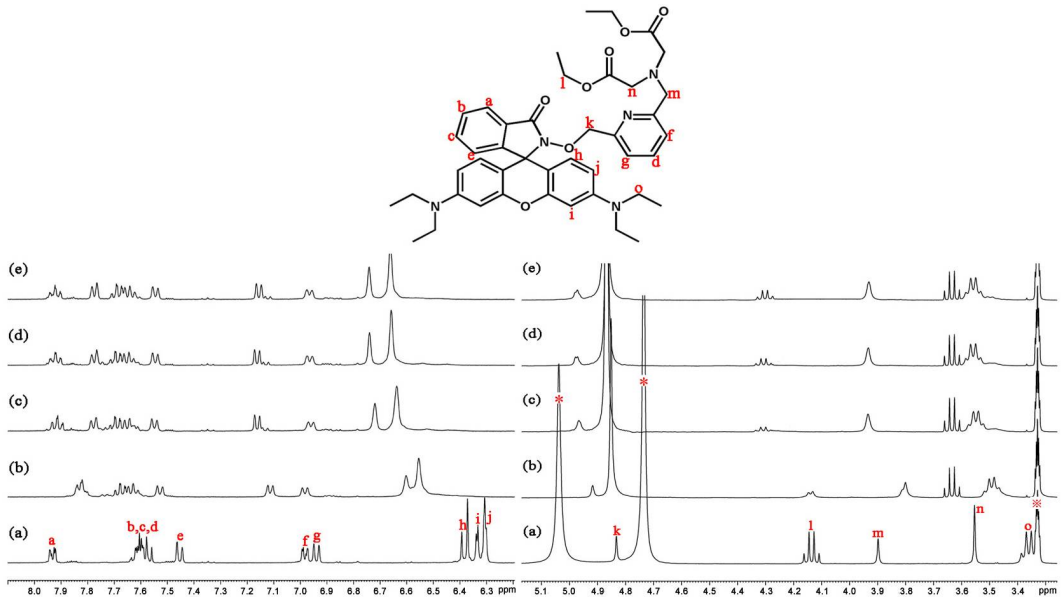

Fig. S14. ^{1}H NMR (400 MHz) spectral changes of **L** (10 mM) in CD_3OD/D_2O (4.5:1) upon addition of $Pb(NO_3)_2$ at 298 K. (a) **L**, (b) **L** + Pb^{2+} (1:0.5), (c) **L** + Pb^{2+} (1:1), (d) **L** + Pb^{2+} (1:2), (e) **L** + Pb^{2+} (1:5), where ∗ denotes the residual proton signal from D_2O and ※ denotes the residual proton signal from CD_3OD.

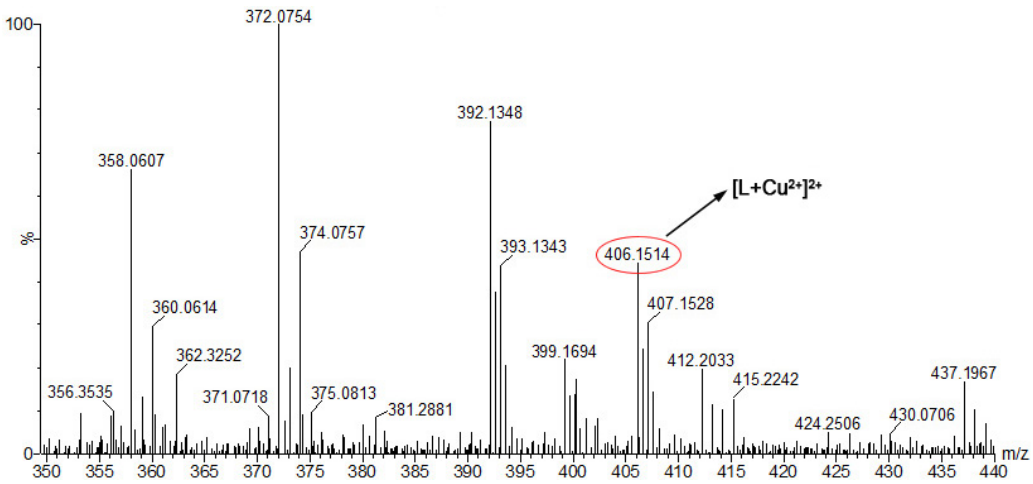

Fig. S15. ESI-MS spectrum of **L** in the presence of $CuCl_2$.

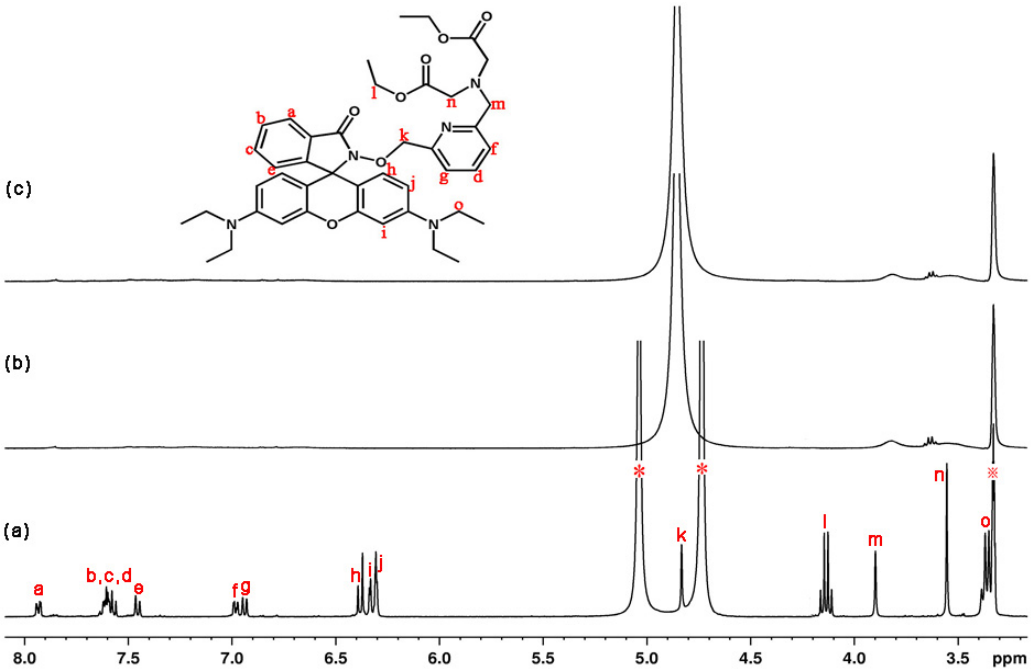

Fig. S16. ^{1}H NMR (400 MHz) spectral changes of **L** (10 mM) in CD_3OD/D_2O (4.5:1) upon addition of $CuCl_2$ at 298 K. (a) **L**, (b) **L** + Cu^{2+} (1:0.5), (c) **L** + Cu^{2+} (1:1), where ∗ denotes the residual proton signal from D_2O and ※ denotes the residual proton signal from CD_3OD.

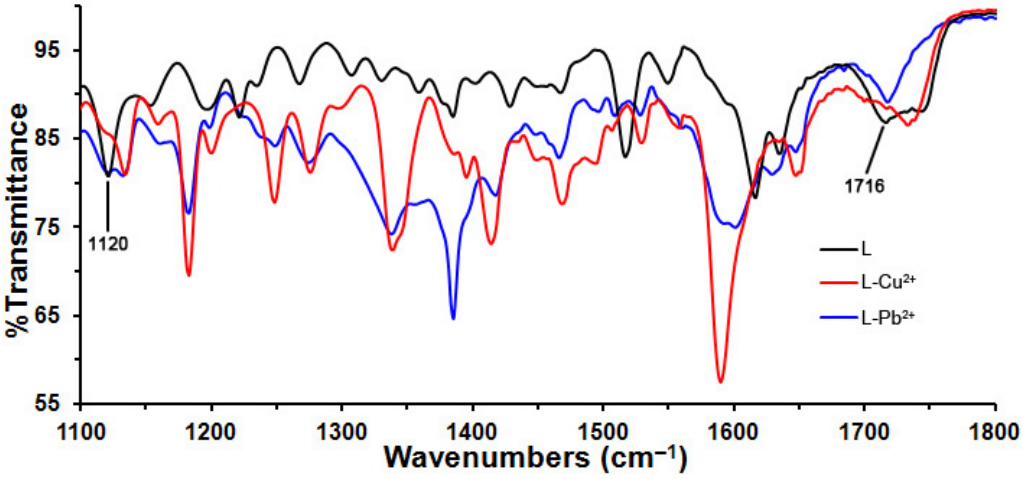

Fig. S17. IR spectra of **L**, **L**-Cu^{2+} and **L**-Pb^{2+}.

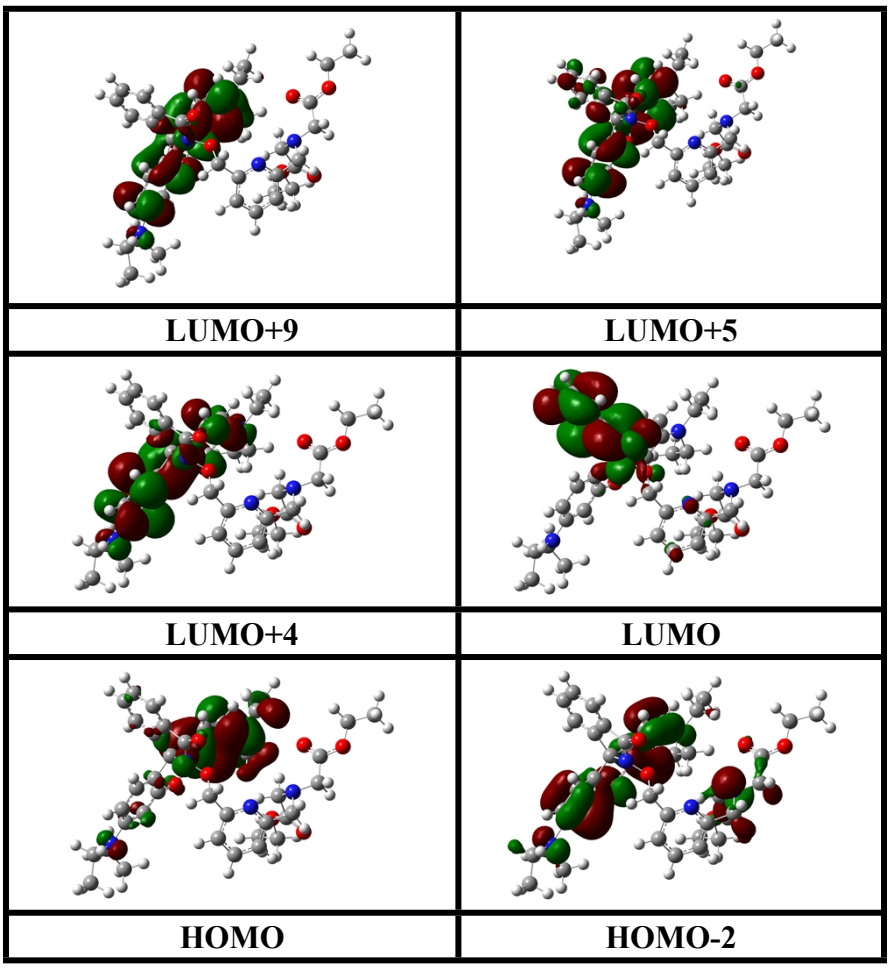

Fig. S18. Frontier molecular orbitals of **L**.

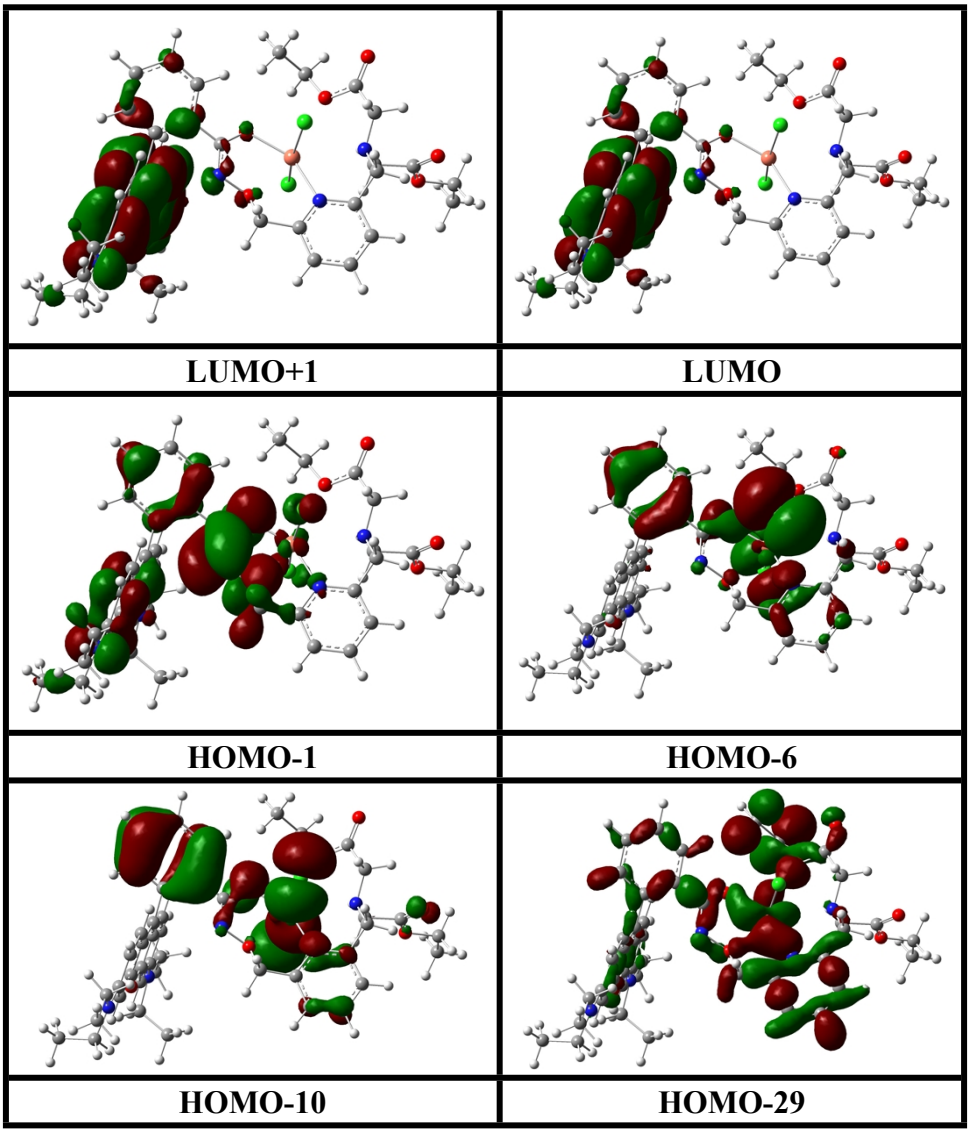

Fig. S19. Frontier molecular orbitals of complex **L**-Cu^{2+}.

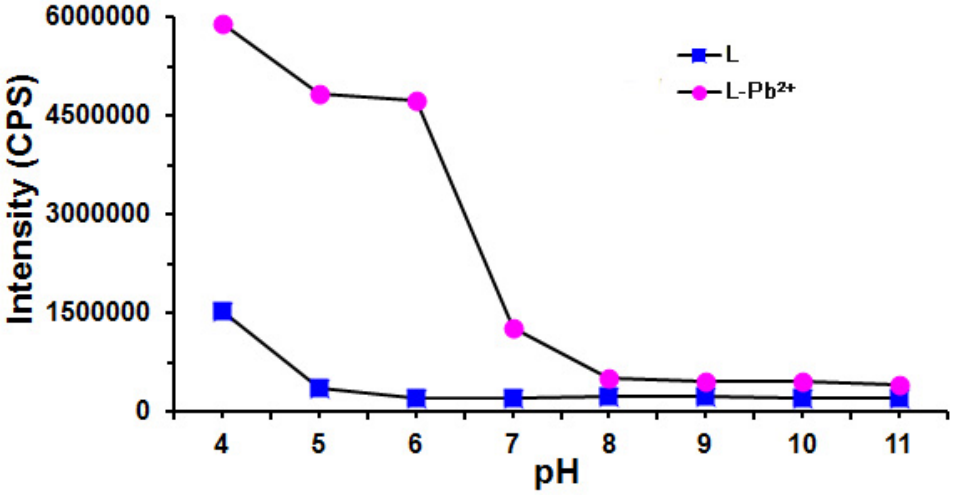

Fig. S20. Fluorescence intensity at 576 nm of **L** (10 μM) measured with 10 equiv Pb^{2+} and without Pb^{2+} in 10 mM HEPES buffer (containing 1% CH_3CN, v/v) at various pH values. The excitation wavelength was 483 nm. The pH of the solutions was adjusted by addition of NaOH (1 M) or HCl (1 M).

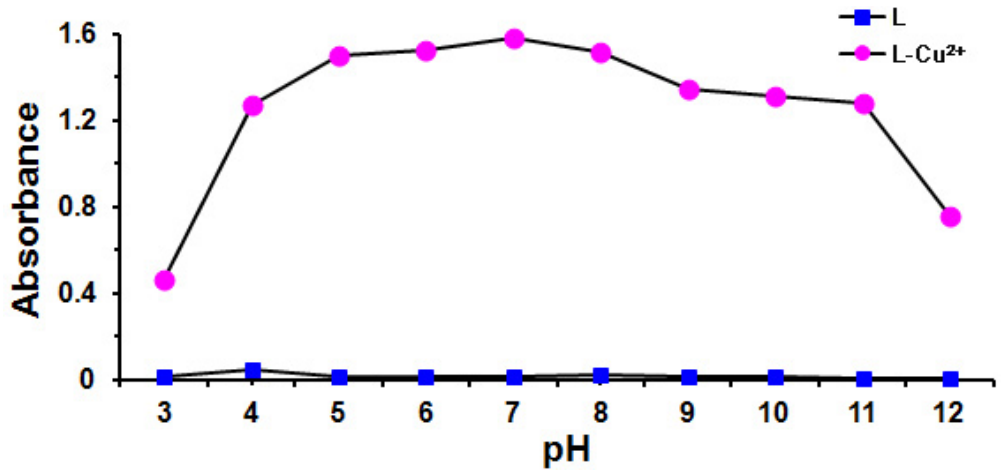

Fig. S21. Absorbance at 567 nm of **L** (10 μM) measured with 10 equiv Cu^{2+} and without Cu^{2+} in 10 mM HEPES buffer (containing 1% CH_3CN, v/v) at various pH values. The pH of the solutions was adjusted by addition of NaOH (1 M) or HCl (1 M).

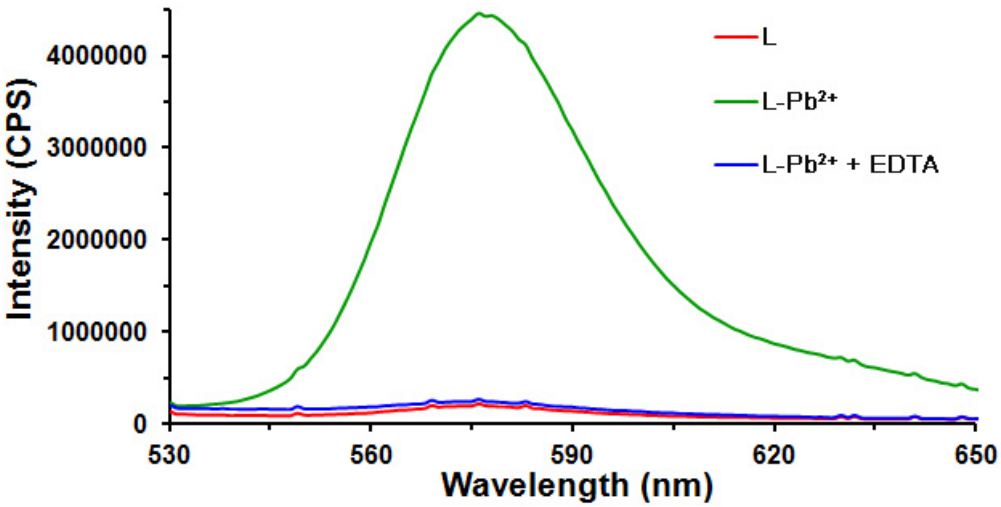

Fig. S22. Reversibility of Pb^{2+} (60 μM) coordination to **L** (10 μM) by EDTA disodium (60 μM) in aqueous HEPES buffer (10 mM, pH 6.5) containing 1% CH_3CN (v/v). The excitation wavelength was 483 nm.

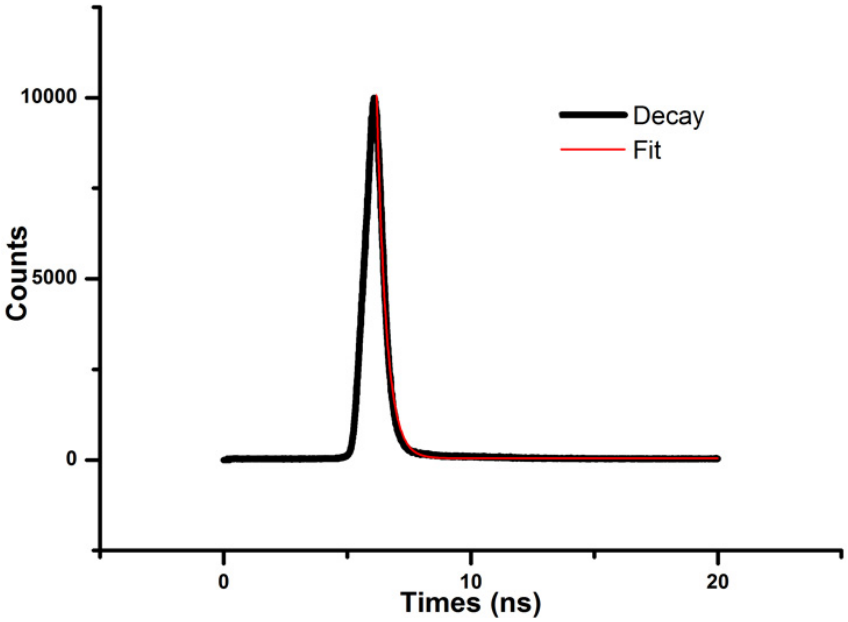

Fig. S23. Fluorescence decay curve of **L** at 576 nm in aqueous HEPES buffer (10 mM, pH 6.5) containing 1% CH_3CN (v/v). λ_{ex} = 483 nm.

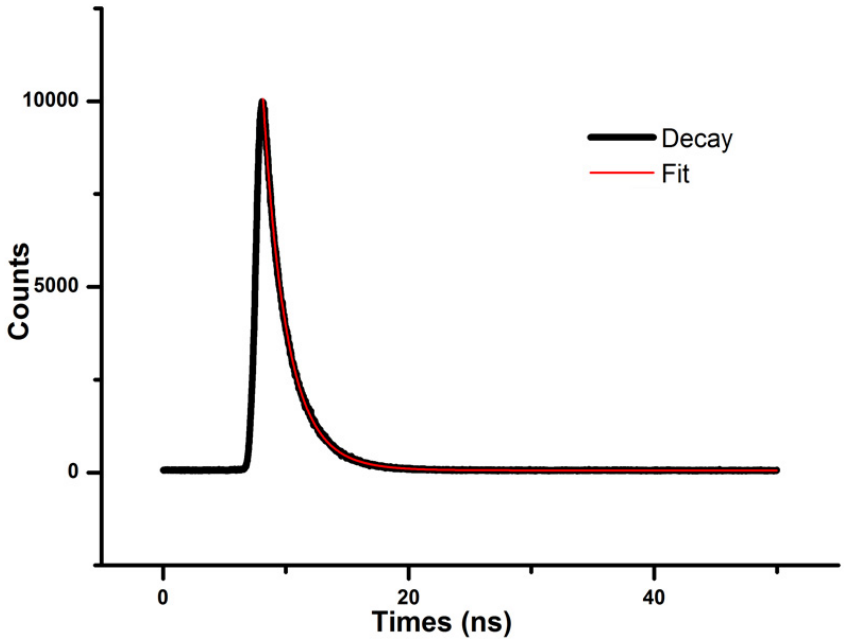

Fig. S24. Fluorescence decay curve of **L** at 576 nm in the presence of 10 equiv Pb^{2+} in aqueous HEPES buffer (10 mM, pH 6.5) containing 1% CH_3CN (v/v). λ_{ex} = 483 nm.

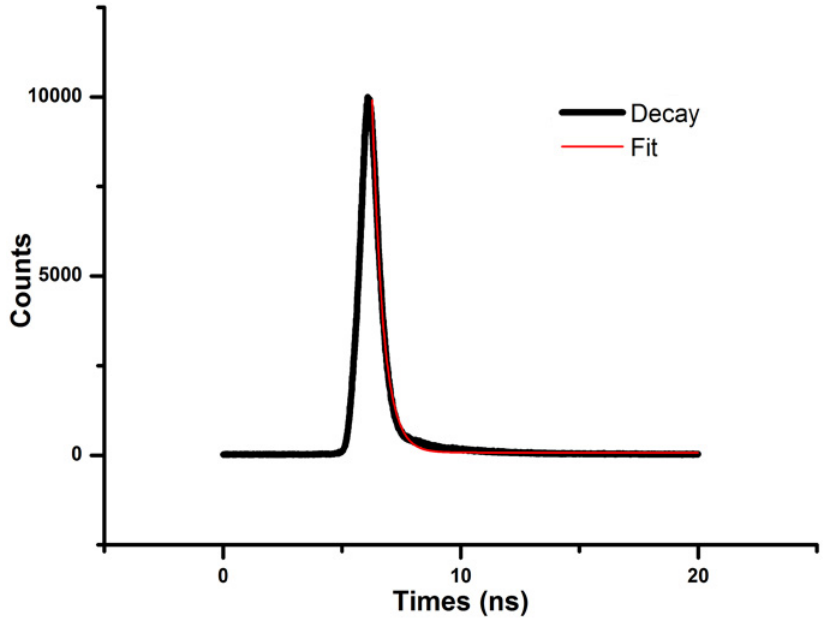

Fig. S25. Fluorescence decay curve of **L**-Pb^{2+} at 576 nm in the presence of 100 equiv EDTA in aqueous HEPES buffer (10 mM, pH 6.5) containing 1% CH_3CN (v/v). λ_{ex} = 483 nm.

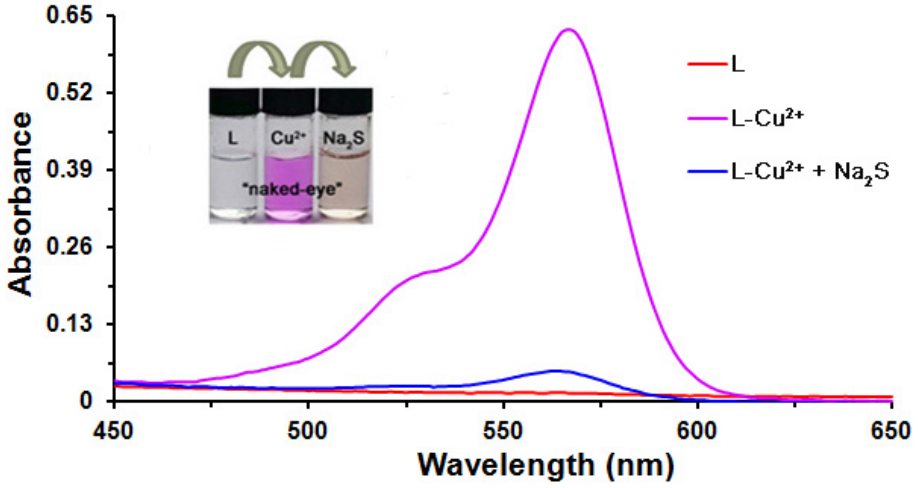

Fig. S26. Reversibility of Cu^{2+} (10 μM) coordination to **L** (10 μM) by Na_2S (20 μM) in aqueous HEPES buffer (10 mM, pH 7.2) containing 1% CH_3CN (v/v).

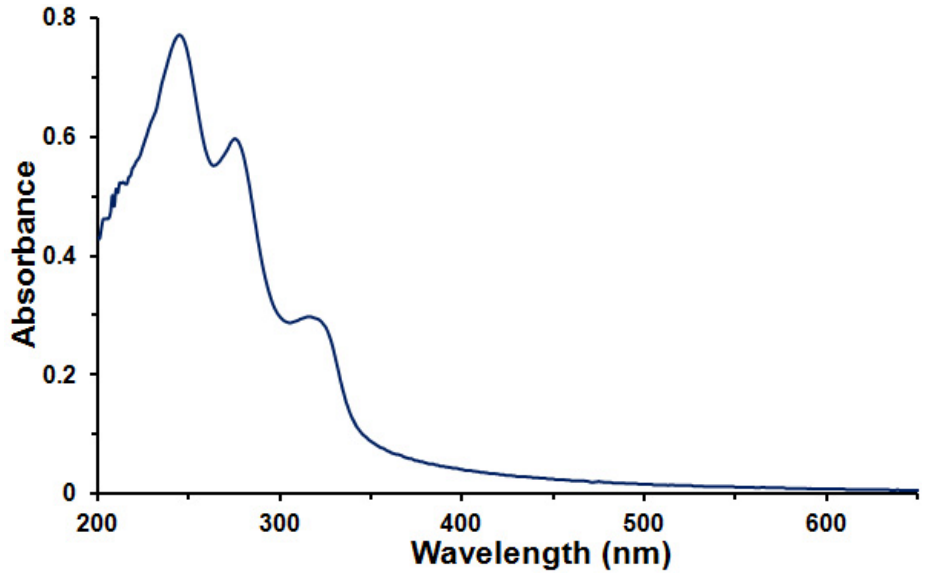

Fig. S27. The absorbance spectra of **L** in aqueous HEPES buffer (10 mM, pH 7.2) containing 1% CH_3CN (v/v).

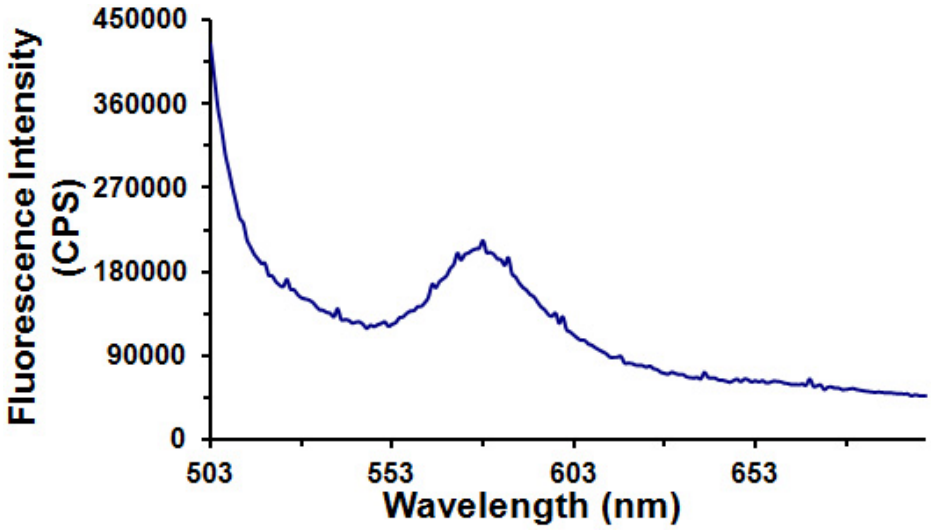

Fig. S28. The fluorescence emission spectra of **L** in aqueous HEPES buffer (10 mM, pH 6.5) containing 1% CH_3CN (v/v). λ_{ex} = 483 nm.

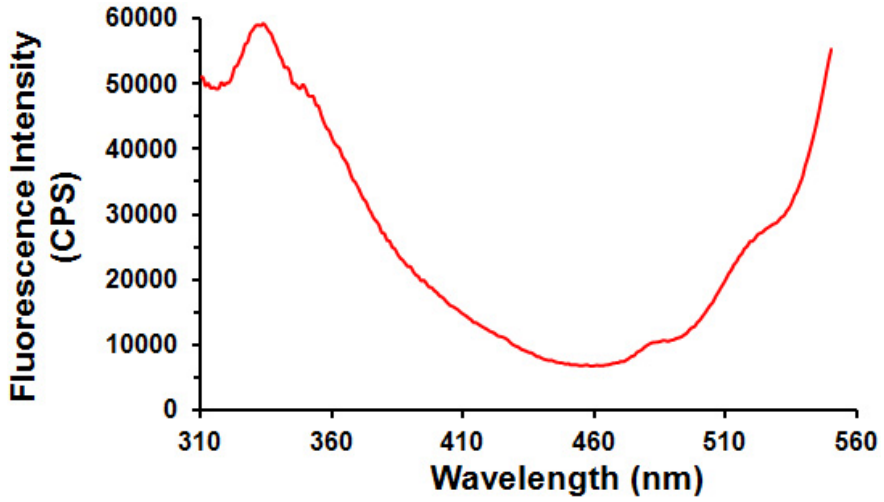

Fig. S29. The excitation spectra of **L** in aqueous HEPES buffer (10 mM, pH 6.5) containing 1% CH_3CN (v/v). λ_{em} = 576 nm.

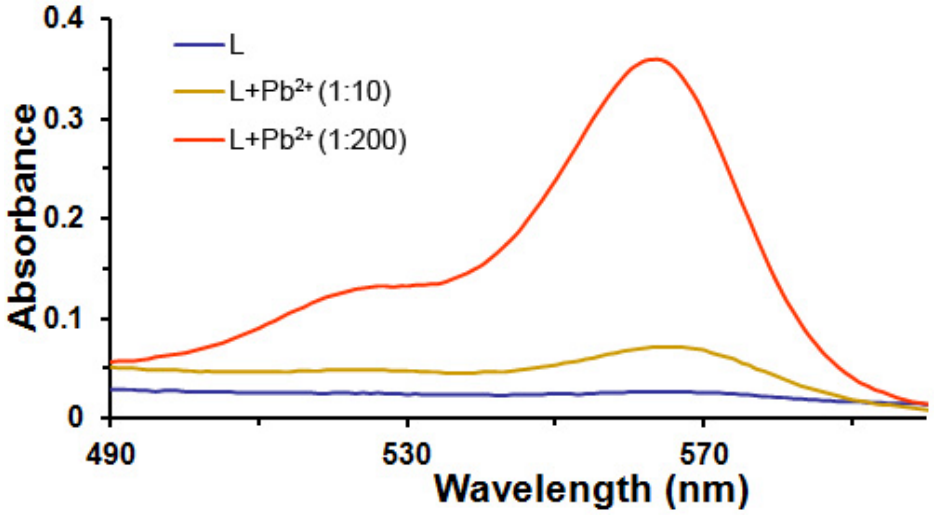

Fig. S30. UV–vis absorption spectra of **L** (10 μM) with addition of Pb^{2+} in aqueous HEPES buffer (10 mM, pH 7.2) containing 1% CH_3CN (v/v).

Table S1. Crystallographic data and structure refinement parameters for complex **L**-Pb^{2+}.

Compound	**L**-Pb^{2+}
Empirical formula	$C_{82}H_{110}N_{14}O_{34}Pb_2$
Formula weight	2250.24
Temperature (K)	293(2)
Crystal system	Triclinic
Space group	$P\bar{1}$
a (Å)	12.1829(4)
b (Å)	14.0906(8)
c (Å)	14.9798(6)
α (°)	63.766(5)
β (°)	77.410(3)
γ (°)	78.245(4)
V (Å^3)	2234.16(17)
Z	1
D_c (Mg/m^3)	1.673
μ (mm^{-1})	3.858
F(000)	1136
Reflns collected	17572
Independent reflns	8315
Completeness	99.8 %
R(int)	0.0589
Refinement method	Full-matrix least-squares on F^2
Data / restraints / parameters	8302 / 3733 / 588
GOF on F^2	1.007
$^aR_1[I>2\sigma(I)]$, wR_2	0.0680, 0.1700
R_1[all data], wR_2	0.0819, 0.1824

$^aR_1=\Sigma||F_o| - |F_c||/\Sigma|F_o|$, $wR_2=[\Sigma[w(F_o^2 - F_c^2)^2]/\Sigma w(F_o^2)^2]^{1/2}$

Table S2. Selected bond lengths (Å) and angles [deg] for complex **L**-Pb^{2+}.

bond lengths (Å)			
Pb(1)–O(7)	2.387(6)	Pb(1)–O(7)#1	2.676(5)
Pb(1)–O(1)	2.471(5)	Pb(1)–O(12)	3.023(10)
Pb(1)–N(4)	2.643(7)	Pb(1)–O(4)	2.924(7)
Pb(1)–N(5)	2.660(7)	Pb(1)–O(3)	2.921(6)
bond angles (°)			
O(7)–Pb(1)–O(1)	70.92(18)	N(5)–Pb(1)–O(4)	58.0(2)
O(7)–Pb(1)–N(4)	102.0(2)	N(5)–Pb(1)–O(12)	83.4(3)
O(1)–Pb(1)–N(4)	73.5(2)	N(4)–Pb(1)–O(3)	61.1(2)
O(7)–Pb(1)–N(5)	64.2(2)	N(4)–Pb(1)–O(4)	105.9(2)
O(1)–Pb(1)–N(5)	106.7(2)	N(4)–Pb(1)–O(12)	67.0(3)
N(4)–Pb(1)–N(5)	63.8(2)	O(1)–Pb(1)–O(4)	160.6(2)
O(7)–Pb(1)–O(7)#1	66.1(2)	O(1)–Pb(1)–O(3)	59.8(2)
O(1)–Pb(1)–O(7)#1	73.30(18)	O(1)–Pb(1)–O(12)	129.1(3)
N(4)–Pb(1)–O(7)#1	146.8(2)	O(7)#1–Pb(1)–O(3)	101.9(2)
N(5)–Pb(1)–O(7)#1	126.59(19)	O(7)#1–Pb(1)–O(4)	105.1(2)
O(7)–Pb(1)–O(4)	90.5(2)	O(7)#1–Pb(1)–O(12)	139.2(3)
O(7)–Pb(1)–O(3)	130.6(2)	O(3) –Pb(1)–O(4)	137.6(2)
O(7)–Pb(1)–O(12)	146.8(3)	O(4)–Pb(1)–O(12)	64.8(3)
N(5)–Pb(1)–O(3)	124.8(2)	O(3)–Pb(1)–O(12)	73.3(3)

Symmetry transformations used to generate equivalent atoms: #1 $-x + 1, -y, -z + 1$.

Table S3. The contribution of each orbital transitions to the lowest energy transition of **L** and **L**-Cu^{2+}.

electronic transition	**L** oscillator strength (f)	electronic transition	**L**-Cu^{2+} oscillator strength (f)
HOMO→LUMO+4	0.1434	HOMO−10→LUMO+1	0.4619
HOMO−2→LUMO	0.1434	HOMO−6→LUMO+1	0.4619
HOMO−2→LUMO+5	0.2312	HOMO−1→LUMO	0.4295
HOMO→LUMO+9	0.7335	HOMO−29→LUMO+1	0.4295

Table S4. Fluorescence decay time constants of **L**, **L**-Pb^{2+} and **L**-Pb^{2+}-EDTA.

	A_1	τ_1/ns	A_2	τ_2/ns	$<\tau>$/ns	χ^2
L at 576 nm	50%	0.384	50%	0.384	0.384	1.024
L-Pb^{2+} at 576 nm	40%	2.597	60%	1.608	2.004	1.163
L-Pb^{2+}-EDTA at 576 nm	50%	0.467	50%	0.467	0.467	1.144

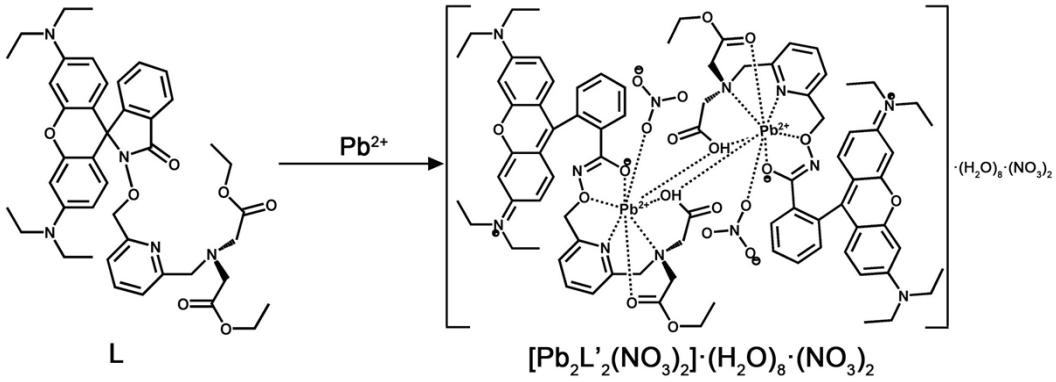

Scheme S1. The schematic representation the transformation process of **L** structure upon complexation to Pb^{2+}, where **L**' represented the ester hydrolyzed product of **L**.